

TERAHERTZ BOW-TIE DIODE BASED ON ASYMMETRICALLY SHAPED AlGa_N/Ga_N HETEROSTRUCTURES

J. Jorudas^a, D. Seliuta^a, L. Minkevičius^a, V. Janonis^a, L. Subačius^a,

D. Pashnev^a, S. Pralgauskaitė^a, J. Matukas^a, K. Ikamas^b, A. Lissauskas^b, E. Šermukšnis^c,

A. Šimukovič^c, J. Liberis^c, V. Kovalevskij^d, and I. Kašalynas^{a,b}

^aTerahertz Photonics Laboratory, Center for Physical Sciences and Technology, Saulėtekio 3, 10257 Vilnius, Lithuania

^bInstitute of Applied Electrodynamics and Telecommunications, Vilnius University, Saulėtekio 3, 10257 Vilnius, Lithuania

^cFluctuation Research Laboratory, Center for Physical Sciences and Technology, Saulėtekio 3, 10257 Vilnius, Lithuania

^dExperimental Nuclear Physics Laboratory, Center for Physical Sciences and Technology,
Saulėtekio 3, 10257 Vilnius, Lithuania

Email: irmantas.kasalynas@ftmc.lt

Received 3 October 2023; accepted 3 October 2023

Asymmetrical shaping of AlGa_N/Ga_N heterostructures containing a conductive layer of two-dimensional electron gas (2DEG) was used for the development of bow-tie (BT) diodes for room temperature terahertz (THz) detection. Considering operation of the THz BT diode in the unbiased mode as preferable for practical applications, we investigated the diodes with an obvious asymmetry of *IV* characteristics, which was found to be more pronounced with the decrease of an apex width, resulting in the sensitive THz detection. A nonuniform heating of carriers in a metalized leaf of the BT diode was attributed as the main mechanism that caused the rectification of THz waves. The responsivity and noise-equivalent power (NEP) at the fundamental antenna frequency of 150 GHz were up to 4 V/W and 2 nW/√Hz, respectively. Such high sensitivity of BT diodes allowed us to measure for the first time the response spectrum of the asymmetric BT antenna demonstrating fundamental and higher order resonances in good agreement with finite-difference time-domain simulation data in a broad spectrum range. The detailed investigation of the low- and high-frequency noise characteristics of AlGa_N/Ga_N BT diodes revealed that only thermal noise needs to be considered for the unbiased operation, the value of which was relatively low due to a high density of 2DEG enabling low resistivity values. Moreover, we observed that the responsivity of BT diode scales with its resistance, revealing that tapering of the diode apex below a few microns could be ineffective in applications which require low NEP values.

Keywords: THz bow-tie diode, AlGa_N/Ga_N heterostructure, 2DEG, asymmetrical BT antenna

1. Introduction

The evolution of terahertz (THz) science and technology enable new applications in wireless communication, spectroscopic imaging, chemical and biological sensing, but still requires the development of fast, sensitive and room-temperature THz detectors [1, 2]. Of particular interest are semiconductor based sensors which can be integrated on-chip implementing scalable planar schemes [3–5]. The detectors based on hot-electron effects are attractive due to their high sensitivity and de-

tection capabilities achieved in the broadband spectrum [6–8]. In such devices, the rectification of electromagnetic waves is achieved by thermoelectric effects which are the result of the formation of free-carrier temperature gradients due to asymmetric conditions such as geometrical shaping, doping profile, contact and coupling characteristics [9–11].

Initially, the hot-carrier-based detector was developed as a small area whisker-contact of metal-semiconductor structure, where high-frequency electric fields used to be concentrated in a small

region of active material [12]. Years later, the planar structures of n-n⁺-GaAs possessing a high electron mobility were developed by shaping layers in a bow-tie (BT) antenna geometry and demonstrating the sensor operation in the GHz and THz frequency bands [9]. As a further improvement, the InGaAs layer on the InP substrate was selected together with a more asymmetric planar geometry and a complete one leaf metallization of the diode, representing the form of an asymmetric BT antenna [13]. All these THz sensors were found to be well suited in compact spectroscopic imaging systems operating in the direct detection scheme [14]. The response speed of BT diodes was found to be below nanoseconds [15], which allowed one to record amplitude and phase images quickly in the heterodyne configuration [16]. Different approaches were tested to increase the detector sensitivity such as using a modulation-doped AlGaAs/GaAs heterostructure with a 2D electron gas (2DEG) layer [17], applying the voltage/current bias to BT diode electrodes [14], and providing a field-plate (short-gate) over active part of the BT diode [18, 19]. Moreover, the Fermi-level managed barrier (FMB) diode based on the InGaAs lattice matched to the InP structure was proposed for low-noise THz wave detection at room temperature [20]. In addition, researchers have proposed the high sensitivity In_{0.53}Ga_{0.47}As photodetector [21] as well as the heterostructured low-barrier diode (HLBD) composed of a composition-graded lattice-matched AlGaInAs triangular barrier in the GaAs/AlGaAs system [22] for room-temperature sensitive sub-THz detection.

The heterostructure-based sensor benefits from the fact that the electron energy relaxation is dominated by the ballistic outflow, which allows one to reduce the electron cooling time and, therefore, the response time of the sensor [23]. The sensitivity and noise-equivalent power (NEP) of BT diodes based on the GaAs material system were found to be up to 10 V/W and down to 4 nW/√Hz, respectively [14, 16]. Utilizing the strong built-in internal electric fields achieved by a specific growth condition of the InGaAs layer on the InP substrate enabled a significant reduction of NEP down to the value of 200 pW/√Hz at a selected frequency of 0.6 THz [24]. Meanwhile, sensitive HLBDs and photodetectors demonstrated a significantly bet-

ter responsivity and NEP values, which at the frequency of around 180 GHz reached up to 6000 and 515 V/W and lower than 0.6 and 20 pW/√Hz, respectively [21, 22].

In this work, we investigated the BT diodes developed of commercially available AlGaIn/GaN heterostructures dedicated to high-electron mobility transistor (HEMT) applications. Compared to previously used GaAs-material systems, the selected material has an advantage of a higher electron density, which is useful for a better match between the THz sensor and asymmetric BT antenna impedances [7]. In addition, the short momentum relaxation time of electrons ensures the THz coupling to the 2DEG layer [25, 26]. Furthermore, good ohmic contacts to 2DEG in AlGaIn/GaN heterostructures can be obtained without the heavy doping of semiconductor layers. This simplifies the interpretation of THz signals caused by carrier heating in the asymmetrically necked contact and semiconductor materials if one takes into account self-heating effects of both ohmic contacts and 2DEG layer, observed even under short-duration (only 100 ns) and low-duty-cycle (only 10⁻⁵) pulsed electric fields [27].

In this work, we attributed the detected THz signals to the nonuniform heating of carriers in the area of a metallized leaf of the BT diode, resulting in the responsivity and NEP values at 150 GHz frequency and room temperature to be up to 4 V/W and 2 nW/√Hz, respectively. A sufficiently high sensitivity of the BT diode allowed us to record the emission spectrum of the frequency-domain spectrometer source, providing THz powers up to 1 μW in the free space. As a result, the asymmetric BT antenna response spectrum was recorded for the first time. Due to the different device and electrode shaping shown in the designs of Fig. 1(a) and in Refs. [13, 14], the AlGaIn/GaN BT diodes revealed a significantly different frequency characteristic in comparison to that of the InGaAs-BT diodes, results of which will be reported elsewhere. In addition, the noise characteristics and the optical responsivity dependence from the apex width and the resistance of BT diode were investigated. The results indicate that the hot electron effects in the metallized leaf are responsible for the optimal operation of THz BT diodes even without an external bias.

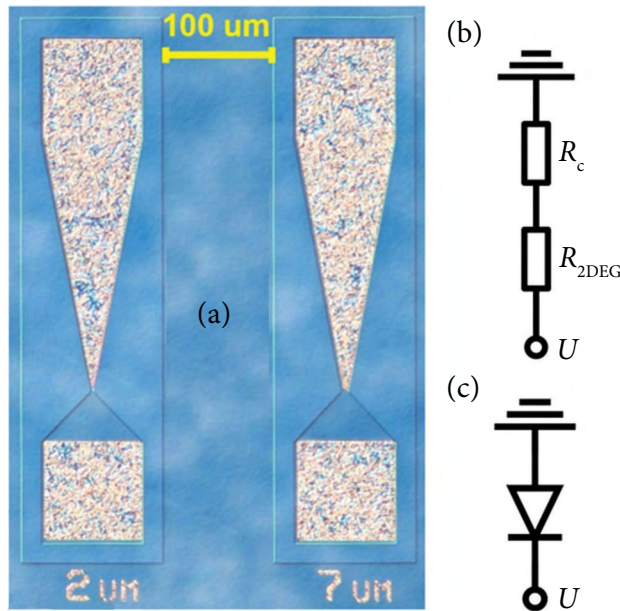


Fig. 1. (a) Nomarski-contrast microscope image of the BT diodes fabricated of asymmetrically shaped AlGaIn/GaN heterostructures with a conductive 2DEG layer. The total length of diode is $500 \mu\text{m}$, the width is $100 \mu\text{m}$, and the length of metallized and unmetallized heterostructure leaf is 250 and $50 \mu\text{m}$, respectively. The apex width of shown diodes is 2 and $7 \mu\text{m}$ (as labelled). (b) Suggested equivalent circuit and (c) the symbol of the BT diode, where the resistance R_c stands for the metallized and $R_{2\text{DEG}}$ for the unmetallized leaf, which both could be sensitive to the magnitude of the applied electric field.

2. Samples

Microscope image of two fabricated BT diodes with the apex width of 2 and $7 \mu\text{m}$ is shown in Fig. 1(a). The samples were fabricated of AlGaIn/GaN heterostructures grown on a $500 \mu\text{m}$ thick semi-insulating 6H-SiC substrate which were kindly provided for the research by *TopGaN* (www.topganlasers.com) company. The structure was composed of $1 \mu\text{m}$ thick unintentionally doped GaN buffer and 19 nm thick $\text{Al}_{0.25}\text{Ga}_{0.75}\text{N}$ barrier layers with a 1 nm thick AlN spacer in between. A conductive channel of 2DEG is localized below the AlN spacer in the top part of the buffer layer. DC conductivity and Hall effect measurements at room temperature revealed 2DEG density and low-field mobility values of about $8.3 \times 10^{12} \text{ cm}^{-2}$ and $1.9 \times 10^3 \text{ cm}^2/\text{Vs}$, respectively. From these data the sheet resistivity of the 2DEG layer was estimated to be of about 400Ω per square.

The mesas of asymmetrically shaped AlGaIn/GaN heterostructures were developed either by optical photolithography and dry plasma etching or by implantation of Al ions. The ohmic contacts (Ti/Al/Ni/Au: $30/90/20/100 \text{ nm}$) were processed on top of the mesa using e-beam metal evaporation followed by rapid thermal annealing in the N_2 environment. The metallized leaf is used to concentrate electric field in the apex area, while the unmetallized leaf, a fragment of mesa between two electrodes, is designed as an active part of the sensor, generating a DC signal when exposed to THz radiation. The performance of all BT diodes was investigated in the unbiased mode operation at room temperature unless otherwise specified.

3. Results

Two types of the IV characteristics of AlGaIn/GaN based BT diodes were found after chip fabrication using the same recipe for ohmic contacts [28, 29]. In the first case, the resistance of the metallized BT antenna leaf was found to be insensitive to the magnitude of the applied electric field, $R_c \approx \text{const}$, resulting in the symmetric IV characteristic of the BT diode. The typical results are shown in Fig. 2 by grey colour short-dash lines. Such type of BT diodes without a bias demonstrated relatively small THz signals

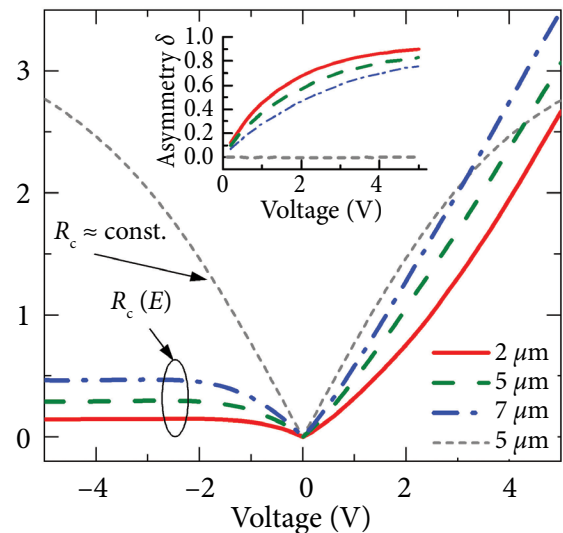


Fig. 2. Current–voltage characteristics of the fabricated BT diodes with different width of the apex (indicated in microns) demonstrating the resistance of metallized leaf's weak and strong dependence on applied electric field (labelled as $R_c \approx \text{const}$ and $R_c(E)$, respectively). Inset is the asymmetry factor according to Eq. (1).

and responsivity values (see data shown in Fig. 3 by circle symbols) [29].

In another group, the BT diodes demonstrated the resistance of contacts made to be sensitive to the applied electric field $R_c(E)$. These BT diodes demonstrated an obvious asymmetry of IV characteristics, which was more pronounced with the decrease of apex width. The measurement results for BT diodes with different apex sizes are shown in Fig. 2. Here more pronounced carrier heating in the shaped sub-contact area in comparison to the 2DEG channel can be identified [12, 27]. These BT diodes demonstrated a sensitive THz detection in the unbiased regime, thus, only data for those will be discussed further. It is worth to note that the behaviour in the DC regime and the THz performance of such sensors were found to be very similar to those of InGaAs-BT diodes [14], and such facts can be used in the future for the side-by-side comparison of different types of BT diodes.

The transmission line method (TLM) was used to investigate the contact resistance of devices on each AlGaIn/GaN chip after the fabrication process. The contact resistance R_c and the specific contact resistivity ρ_c were measured using rectangular shape test TLM structures of 250 μm wide contacts separated by a distance from 3 to 65 μm , revealing the values down to $1 \Omega \times \text{mm}$ and $2 \cdot 10^{-5} \Omega \times \text{cm}^2$, respectively. However, electrode shaping for BT diodes down to the sub-micron size can also modify the contact resistance. Thus, after the device fabrication only the IV characterization of BT diodes and test TLM structures allowed us to reveal whether the resistance of tapered metallized leaf was dependent on DC voltage or not.

The polarity of bias voltage is determined in respect to the tapered electrode (metallized leaf) which was kept grounded in all experiments. The asymmetry factor of DC currents was defined as [14]

$$\delta = \frac{I_+ - I_-}{I_+ + I_-}, \quad (1)$$

where I_+ and I_- are the BT diode current measured at positive and negative values of the same bias voltage, respectively. The asymmetry factor of different BT diodes is shown in the inset of Fig. 2. The asymmetry of IV curves for the BT diodes with $R_c(E)$ was attributed to the electron heating in the sub-contact area of the metallized leaf. The asymmetry of the current flow is a result of the nonuniform heating of carri-

ers in the vicinity of the apex [7]. Therefore, narrowing of the apex leads to higher electric field values in vicinity of the apex resulting in larger values of the asymmetry factor (see the inset of Fig. 2).

The sensitivity of the BT diode was measured using a quasi-optical setup consisting of an RF signal generator operating at 12.5 GHz and an amplifier-multiplier chain (*Virginia Diodes, Inc.*) with a multiplication factor of 12, 24 and 48 for generating oscillations at 150, 300 and 600 GHz, respectively. A Gunn diode oscillator was used to produce radiation at 94 GHz. The THz beam was emitted to the free space through a horn antenna and was collimated with a 90° off-axis parabolic mirror (OAPM) with a focal length of 10 cm and a diameter of 2 inches. The second OAPM of the same type was used to focus the THz beam onto a hemispherical silicon lens of 12 mm in diameter attached to the back side of a wafer with BT diodes. The power reaching the hemispherical silicon lens was 17, 29, 7 and 0.35 mW at 100, 150, 300 and 600 GHz, respectively. The THz signals were recorded using the lock-in technique.

The responsivity of BT diodes with various apex sizes was measured. The averaged results for 150 GHz frequency are shown in Fig. 3. The responsivity was found by dividing the induced signal voltage over the power of THz beam incident on the BT diode

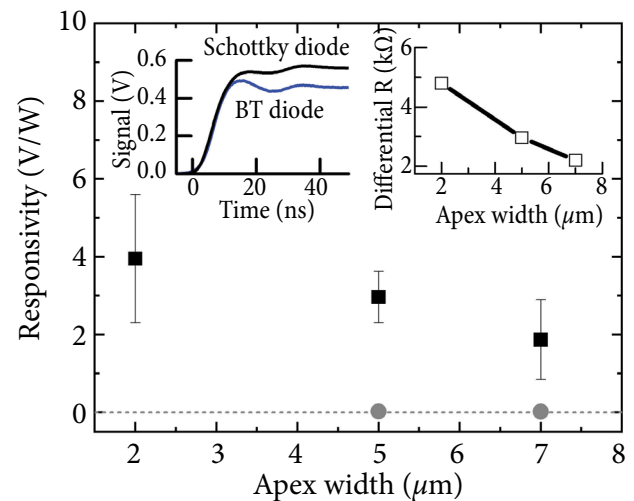


Fig. 3. Measured responsivity dependence on the apex width: squares stand for the BT diodes with $R_c(E)$ and circles for the BT diodes with $R_c \approx \text{constant}$ (see also Fig. 2). Right-hand-side inset: the differential resistance of BT diode versus apex width. Left-hand-side inset: comparison of the response speed of BT diode versus Schottky diode.

(power density). As expected, there is a decrease in the voltage sensitivity with an increase in the neck width of the diode. The deviation range of responsivity values was largest for a group of BT diodes with the apex size of $2\ \mu\text{m}$ independently on the detected THz frequency. It is worth noting that the differential resistance follows a similar trend – decreases with the neck width as it is seen in the right-hand-side inset of Fig. 3.

The detector speed was determined by using mw-field pulses [28]. The response speed of the AlGaIn/GaN BT diode was compared to that of the Schottky barrier diode. The measured pulsed traces are shown in the left-hand-side inset of Fig. 3. The BT diodes showed sub-nanosecond responsivity in a similar manner as the BT diodes developed previously of InGaAs-material [15].

The responsivity spectrum of the BT diodes was measured using the monochromatic radiation of a frequency-domain THz spectrometer TeraScan 780 (*Toptica, Inc.*). The THz beam was electrically modulated at 500 Hz and detected with a lock-in amplifier. The collimating and focusing optics were the same as described previously. The peak THz power of this source was found to be at around the 100 GHz frequency with a value of about $1\ \mu\text{W}$, and the sensitivity of developed BT diodes was sufficient to record such power levels.

The normalized responsivity spectrum of the BT diode with a $2\ \mu\text{m}$ wide apex is shown in Fig. 4. The results obtained using a Gunn oscillator and VDI multiplier chains are also shown by dots. As seen, the data obtained from both experiments show a good agreement. To study the dynamic range of the BT diodes, we gradually attenuated the THz power and measured the resulting voltage signal. The detected signal grew linearly with the power across the range of about 6 orders of magnitude.

The NEP of the detectors is defined as the ratio between the voltage noise and the responsivity. The data of NEP for the AlGaIn/GaN BT diodes are shown in the inset of Fig. 4. For the unbiased operation, only the thermal noise is considered which is relatively low in the AlGaIn/GaN diodes since a high 2D electron density leads to low resistivity values. The NEP dependence on the apex width was found to be relatively weak. The lowest NEP values were obtained at frequencies close to the resonance of BT antenna, with values down to $2\ \text{nW}/\sqrt{\text{Hz}}$ at an apex width of $2\ \mu\text{m}$.

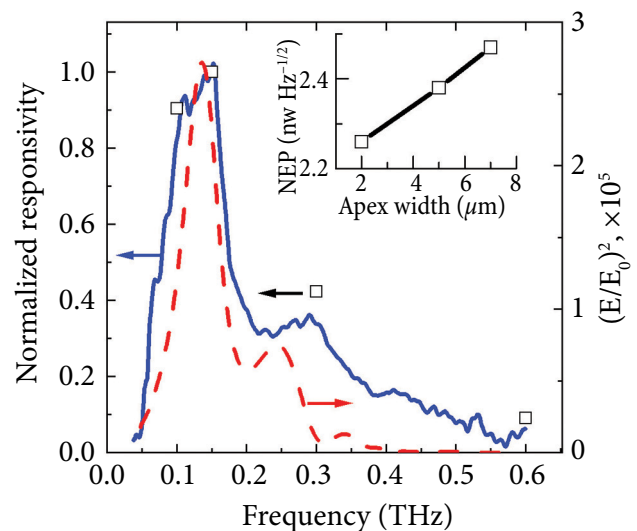


Fig. 4. Responsivity of the BT diode: a solid line shows frequency domain spectroscopy data, dots are the characterization at specific frequencies delivered by Gunn oscillator and frequency multiplier chains, and a dashed line shows the calculated electric field enhancement factor. Apex width of the BT diode is $2\ \mu\text{m}$. Inset: NEP of bow-tie diodes at 150 GHz versus apex width.

Finite-difference time-domain simulations were used to find the electric field amplitude distribution in the plane of the BT diode close to the resonant frequency of the THz antenna. The typical results are shown in Fig. 5. In the inset, the colour coding of electric field amplitudes is used to present data. The surface electric field at the antenna apex was calculated modelling a gold on GaN substrate attached to a silicon lens. For comparison, we plot the square of the electric field enhancement factor, assuming that the electron temperature is proportional to the squared electric field amplitude. The results are shown in Fig. 4.

Comparing the experimental and calculated spectra, one can see that the fundamental resonance of the BT antenna is at the frequency of about 150 GHz. The second resonance is observed in the spectrum slightly below 300 GHz. A reasonable agreement between the measured and calculated spectra is achieved; however, the measured responsivity peak was a bit wider, and the second-order resonance was noticeably attenuated compared to the spectrum of the calculated electric field intensity. A possible explanation could be losses introduced by bond wire connections, which are not taken into account in the calculations.

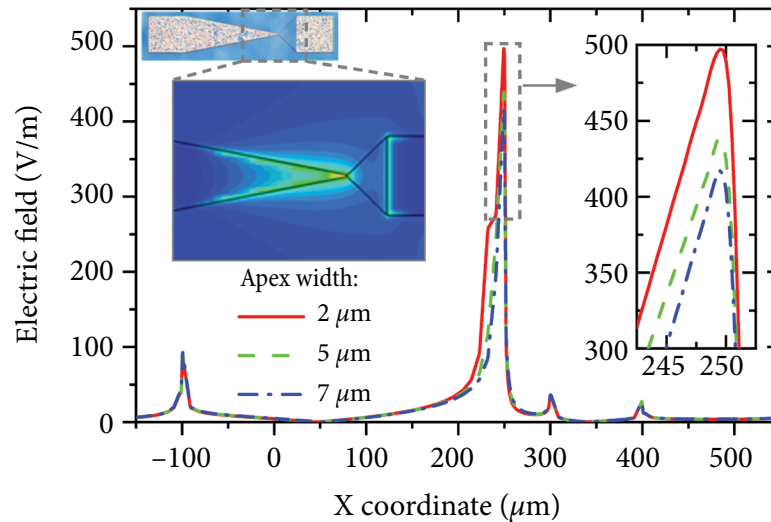


Fig. 5. Modelled surface electric field distributions for the BT diodes with different apex widths. Insets show the characteristic 2D surface electric field distribution and the enlarged plot area near the maximum electric field values.

As seen from Fig. 5, the asymmetric geometry of the BT antenna leads to a strong localization of the THz electric field in the vicinity of the apex and antenna tip. Because of the asymmetry in the carrier temperature, the carrier diffusion brings the charge carriers from the hotter to the colder part of the tapered leaf. As a result, the voltage signal appears at the ends of the BT diode contacts, eliminating the need for an external bias. The direction of the diffusion current is found to be in accordance with the polarity of the signal corresponding to the thermoelectric force of hot electrons [9, 12]. The metallized contacts serve as planar antenna for the normally incident THz wave polarized along the geometric axis of the BT diode. Dimensions of the tapered electrodes result in the resonance at 150 GHz frequency, at which incident radiation is effectively concentrated into the semiconductor. It is worth noting that the response spectrum of the asymmetric BT antenna was recorded for the first time (see Fig. 4), revealing significantly different frequency characteristics from those of the InGaAs-BT diodes, the results of which will be reported elsewhere. A possible reason could be the difference in shaping of the BT diode electrodes fabricated (see Fig. 1(a)) from those described in Refs. [13, 14].

As expected, the narrowing of the diode apex leads to the enhancement of electric field concen-

tration in the metallized leaf tip and apex area (inset of Fig. 5), resulting in the increase of responsivity values (Fig. 3). It is worth to note that the asymmetric shaping of the 2DEG channel can also lead to another detection mechanism, the bi-gradient electromotive force [9].

In general, the response of the hot carrier detector begins to decrease as the detected frequency approaches the inverse of the momentum relaxation time τ_p [8]. The measured Drude conductivity of 2DEG in the AlGaIn/GaN structures at room temperature revealed that the carrier relaxation time at low electric field was about 0.3 ps [25]. This suggests that the theoretical cut off frequency for BT diodes could be about 1 THz.

The noise investigations are often used for a more detailed assessment of the quality of THz detector and materials. The results of low-frequency noise measurements at different bias voltages are shown in Fig. 6. The noise spectral density dependence on bias voltage is asymmetric similarly to the current–voltage characteristic (see also Fig. 2). The noise intensity is lowest at the zero bias (see the inset in Fig. 6). The noise spectra of the investigated structures comprise the $1/f$ fluctuations with the appearance of some Lorentzian type spectral components at specific temperature values. Low frequency noise characteristics of AlGaIn/GaN BT diodes in the temperature range from 78 to 338 K revealed the influence of the defects as

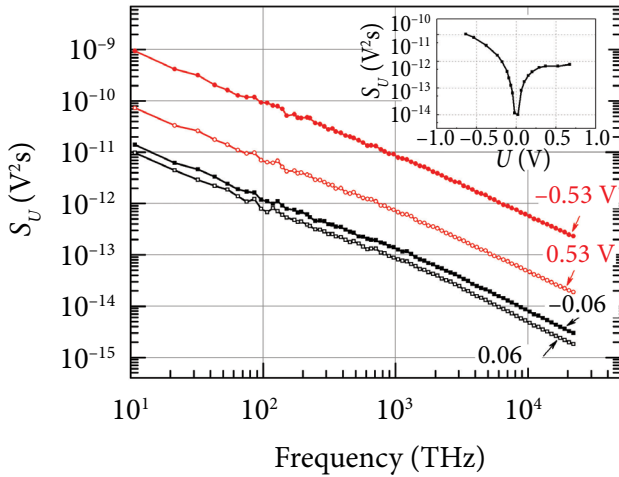


Fig. 6. Voltage noise spectral density at selected bias voltages and the noise spectral density dependence on bias at 1 kHz (in the inset) for the GaN BT diode.

charge carrier capturing centres to the THz detector operation [30]. For the unbiased operation of AlGaIn/GaN BT diodes, only thermal noise needs to be considered, the value of which is relatively low since a high 2DEG density enables low resistivity values.

The microwave noise of the BT diodes and the selected TLM test structures fabricated on the same AlGaIn/GaN sample was investigated using high-frequency measurement setups discussed elsewhere [27]. The excess noise temperature of electrons was measured versus the current density, the values of which were obtained by normalizing the measured charge current to the apex width of BT diode. The results are shown in Fig. 7. The BT diodes demonstrate the asymmetrical behaviour of microwave noise dependent on the bias polarity. The results differed from the characteristics of the rectangular 2DEG layers (TLM resistors), which are shown in Fig. 7 for simplicity with only one polarity. We found that heating of 2D electrons in the BT diode operating in the reverse bias regime is comparable to 2DEG heating in the rectangular shape layer of larger area equipped with large ohmic contacts. Meanwhile, the electron heating was found to be smaller in the BT diode when it operates in the forward bias configuration.

One should note that the BT diodes made of a high electron mobility InGaAs layer [13, 14] showed a similar sensitivity, but the resistance of the samples was more than an order of magnitude larger. The high conductivity of 2DEG channel en-

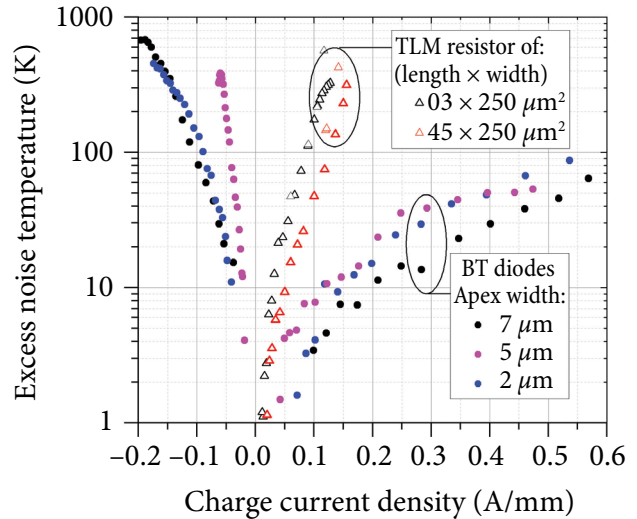


Fig. 7. Excess noise temperature of electrons in the BT diodes with different apex widths (filled-circular symbols) and in the rectangular TLM resistor sample of different indicated size (open-triangular symbols) as a function of charge current density (current normalized to the electrode width).

ables narrowing of the diode apex while maintaining a low diode resistance.

The diode sensitivity at frequencies higher than the fundamental resonance frequency of the BT antenna was found to be almost independent on the apex size. Namely, at 300 GHz frequency, the BT diodes with apexes of 2, 5 and 7 μm demonstrated the average responsivity values of about 1.0, 1.0 and 0.6 V/W, respectively. While at 600 GHz, the sensitivity of BT diodes dropped by another factor of 3 without the pronounced dependence on the apex size. The averaged NEP value of various BT diodes at 300 and 600 GHz frequencies were found at the level of about 10 and 70 $\text{nW}/\sqrt{\text{Hz}}$, respectively.

Although the NEP values of BT diodes are still inferior to those of the state-of-the-art Schottky diodes, FMB diodes and TeraFET detectors [5, 20, 31], from a technological point of view, the fabrication technology of BT diodes is less demanding. Furthermore, the AlGaIn/GaN BT diodes are expected to have an outstanding chemical and physical stability and electrostatic robustness due to the material properties of gallium nitride. While the narrowing of the diode apex leads to the increased sensitivity, we observe that NEP changes very little, since with decreasing the apex width, the total resistance of the BT diode increases. This

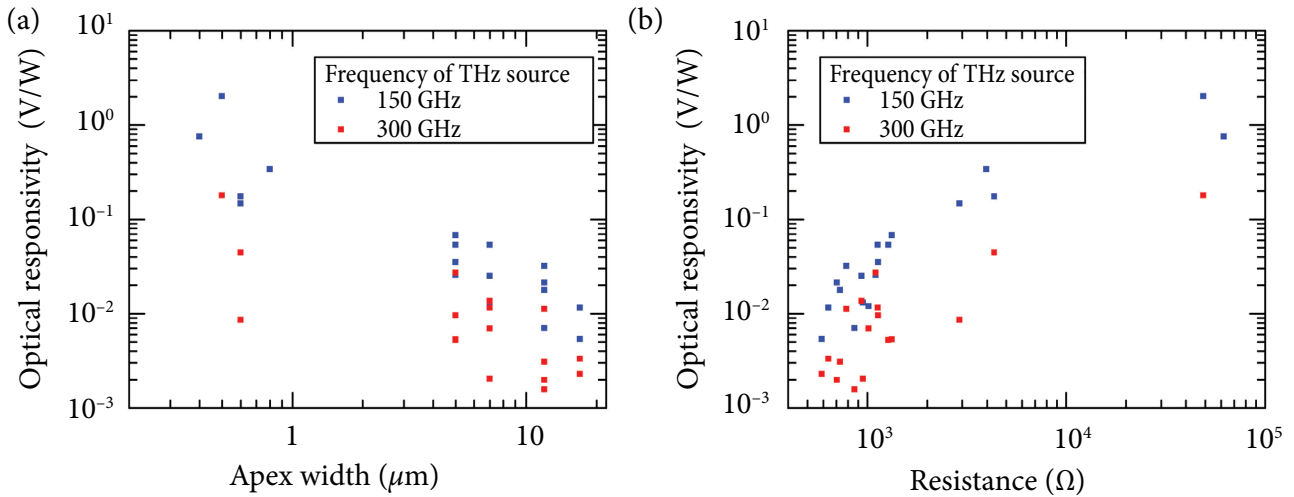


Fig. 8. Responsivity dependence on the apex width (a) and resistance (b) of the BT diode at 150 and 300 GHz frequencies.

suggests that the performance improvement is possible by varying the sheet conductivity of 2DEG layer and by using a different configuration of THz antenna.

Finally, several sets of BT diodes with different apex widths were developed and investigated at the close to resonance frequency of BT antenna in order to obtain more data for statistical analysis. In particular, the planar BT diodes on AlGaIn/GaN HEMT structures were developed considering the variation of apex width from 17 μm down to 0.4 μm [28]. The proposed planar technology is expected to be more suitable for reaching a high range of the THz spectrum as dimensions of the BT diodes can be further scaled down. The optical responsivity dependence on the apex width and the resistance for a number of BT diodes on one chip was measured in the same configuration. The results are shown in Fig. 8. One can see a strong correlation between the resistance and the responsivity values of the BT diode, which depends very little on frequency. Moreover, the responsivity of the BT diode scales nonlinearly with its resistance at values larger than approximately 1000 Ω . Thus, in applications which require low NEP values, tapering the diode apex below a few microns could be ineffective.

4. Conclusions

The BT diodes based on asymmetrically shaped AlGaIn/GaN heterostructures with a 2DEG conductive layer have been investigated as room tem-

perature THz detectors operating in the unbiased mode, preferable for practical applications. Sensitive THz detection was demonstrated by the diodes with an obvious asymmetry of IV characteristics, which was found to be more pronounced with the decrease of apex width. The responsivity and NEP at the fundamental antenna frequency of 150 GHz were up to 4 V/W and down to 2 $\text{nW}/\sqrt{\text{Hz}}$, respectively. Such high sensitivity of BT diodes allowed us to measure for the first time the response spectrum of the asymmetric BT antenna demonstrating fundamental and higher order resonances in good agreement with finite-difference time-domain simulation data in a broad spectrum range. The measured low- and high-frequency noise characteristics of the AlGaIn/GaN BT diodes provide new results about electron heating in the BT diode detector and the unbiased operation for which only thermal noise needs to be considered. Moreover, we observed that the responsivity of the BT diode scales nonlinearly with its resistance, demonstrating that the tapering of the diode apex below the range of a few micrometres could be ineffective in applications which require low NEP values.

Acknowledgements

The authors are sincerely grateful to J. Malakauskaitė and V. Jakštas for their assistance in the sample fabrication, and to P. Prystawko, R. Venckevičius and G. Valušis for fruitful discussions of various aspects of the research. This

work was supported by the Research Council of Lithuania through the ‘T-HP’ Project (Grant No. DOTSUT-184) funded by the European Regional Development Fund according to the supported activity ‘Research Projects Implemented by World-class Researcher Groups’ under Measure No. 01.2.2-LMT-K-718-03-0096.

References

- [1] G. Valušis, A. Lisauskas, H. Yuan, W. Knap, and H.G. Roskos, Roadmap of Terahertz Imaging 2021, *Sensors* **21**, 4092 (2021), <https://doi.org/10.3390/s21124092>
- [2] *THz Communications*, eds. T. Kürner, D.M. Mittleman and T. Nagatsuma (Springer International Publishing, Cham, 2022), <https://doi.org/10.1007/978-3-030-73738-2>
- [3] L. Minkevičius, V. Tamošiunas, K. Madeikis, B. Voisiat, I. Kašalynas, and G. Valušis, On-chip integration of laser-ablated zone plates for detection enhancement of InGaAs bow-tie terahertz detectors, *Electron. Lett.* **50**, 1367–1369 (2014), <https://doi.org/10.1049/el.2014.1893>
- [4] S. Goossens, G. Navickaite, C. Monasterio, S. Gupta, J.J. Piqueras, R. Pérez, G. Burwell, I. Nikitskiy, T. Lasanta, T. Galán, et al., Broadband image sensor array based on graphene–CMOS integration, *Nat. Photonics* **11**, 366–371 (2017), <https://doi.org/10.1038/nphoton.2017.75>
- [5] R. Yadav, F. Ludwig, F.R. Faridi, J.M. Klopff, H.G. Roskos, S. Preu, and A. Penirschke, State-of-the-art room temperature operable zero-bias Schottky diode-based terahertz detector up to 5.56 THz, *Sensors* **23**, 3469 (2023), <https://doi.org/10.3390/s23073469>
- [6] C. Liu, L. Wang, X. Chen, A. Politano, D. Wei, G. Chen, W. Tang, W. Lu, and A. Tredicucci, Room-temperature high-gain long-wavelength photodetector via optical–electrical controlling of hot carriers in graphene, *Adv. Opt. Mater.* **6**, 1800836 (2018), <https://doi.org/10.1002/adom.201800836>
- [7] D. Seliuta, J. Vyšniauskas, K. Ikamas, A. Lisauskas, I. Kašalynas, A. Reklaitis, and G. Valušis, Symmetric bow-tie diode for terahertz detection based on transverse hot-carrier transport, *J. Phys. D* **53**, 275106 (2020), <https://doi.org/10.1088/1361-6463/ab831d>.
- [8] A.M. Cowley and H.O. Sorensen, Quantitative comparison of solid-state microwave detectors, *IEEE Trans. Microw. Theory Tech.* **14**(12), 588–602 (1966), <https://doi.org/10.1109/TMTT.1966.1126337>
- [9] A. Sužiedelis, J. Gradauskas, S. Ašmontas, G. Valušis, and H.G. Roskos, Giga- and terahertz frequency band detector based on an asymmetrically necked n-n+-GaAs planar structure, *J. Appl. Phys.* **93**, 3034–3038 (2003), <https://doi.org/10.1063/1.1536024>
- [10] X. Cai, A.B. Sushkov, R.J. Suess, M.M. Jadidi, G.S. Jenkins, L.O. Nyakiti, R.L. Myers-Ward, S. Li, J. Yan, D.K. Gaskill, T.E. Murphy, H.D. Drew, and M.S. Fuhrer, Sensitive room-temperature terahertz detection via the photothermoelectric effect in graphene, *Nat. Nanotechnol.* **9**, 814–819 (2014), <https://doi.org/10.1038/nnano.2014.182>
- [11] L. Vicarelli, M.S. Vitiello, D. Coquillat, A. Lombardo, A.C. Ferrari, W. Knap, M. Polini, V. Pellegrini, and A. Tredicucci, Graphene field-effect transistors as room-temperature terahertz detectors, *Nat. Mater.* **11**, 865–871 (2012), <https://doi.org/10.1038/nmat3417>
- [12] R.I. Harrison and J. Zucker, Hot-carrier microwave detector, *Proc. IEEE*, **54**(4), 588–595 (1966), <https://doi.org/10.1109/PROC.1966.4778>
- [13] D. Seliuta, I. Kašalynas, V. Tamošiunas, S. Balakauskas, Z. Martunas, S. Ašmontas, G. Valušis, A. Lisauskas, H.G. Roskos, and K. Köhler, Silicon lens-coupled bow-tie InGaAs-based broadband terahertz sensor operating at room temperature, *Electron. Lett.* **42**, 825–827 (2006), <https://doi.org/10.1049/el:20061224>
- [14] I. Kašalynas, R. Venckevičius, D. Seliuta, I. Grigelionis, and G. Valušis, InGaAs-based bow-tie diode for spectroscopic terahertz imaging, *J. Appl. Phys.* **110**, 114505 (2011), <https://doi.org/10.1063/1.3658017>
- [15] I. Kašalynas, D. Seliuta, R. Simniškis, V. Tamošiunas, K. Köhler, and G. Valušis, Terahertz imaging with bow-tie InGaAs-based diode with broken symmetry, *Electron. Lett.* **45**, 833–835 (2009), <https://doi.org/10.1049/el.2009.0336>

- [16] L. Minkevičius, V. Tamošiūnas, I. Kašalynas, D. Seliuta, G. Valušis, A. Lisauskas, S. Boppel, H.G. Roskos, and K. Köhler, Terahertz heterodyne imaging with InGaAs-based bow-tie diodes, *Appl. Phys. Lett.* **99**, 131101 (2011), <https://doi.org/10.1063/1.3641907>
- [17] D. Seliuta, E. Širmulis, V. Tamošiūnas, S. Balauskas, S. Ašmontas, A. Sužiedėlis, J. Gradauskas, G. Valušis, A. Lisauskas, H.G. Roskos, and K. Köhler, Detection of terahertz/sub-terahertz radiation by asymmetrically-shaped 2DEG layers, *Electron. Lett.* **40**, 631 (2004), <https://doi.org/10.1049/el:20040412>
- [18] L. Minkevičius, V. Tamošiūnas, M. Kojelis, E. Žąsinas, V. Bukauskas, A. Šetkus, R. Butkutė, I. Kašalynas, and G. Valušis, Influence of field effects on the performance of InGaAs-based terahertz radiation detectors, *J. Infrared Millim. Terahertz Waves* **38**, 689–707 (2017), <https://doi.org/10.1007/s10762-017-0382-1>
- [19] S. Ašmontas, M. Anbinderis, A. Čerškus, J. Gradauskas, A. Sužiedėlis, A. Šilėnas, E. Širmulis, and V. Umansky, Gated bow-tie diode for microwave to sub-terahertz detection, *Sensors* **20**, 829 (2020), <https://doi.org/10.3390/s20030829>
- [20] H. Ito and T. Ishibashi, Low-noise terahertz-wave detection by InP/InGaAs Fermi-level managed barrier diode, *Appl. Phys. Express* **9**, 092401 (2016), <https://doi.org/10.7567/APEX.9.092401>
- [21] Y. Qu, W. Zhou, J. Tong, N. Yao, X. Xu, T. Hu, Z. Huang, and J. Chu, High sensitivity of room-temperature sub-terahertz photodetector based on $\text{In}_{0.53}\text{Ga}_{0.47}\text{As}$ material, *Appl. Phys. Express* **11**, 112201 (2018), <https://doi.org/10.7567/APEX.11.112201>
- [22] S. Nadar, M. Zaknounge, X. Wallart, C. Coinon, E. Peytavit, G. Ducournau, F. Gamand, M. Thirault, M. Werquin, S. Jonniau, N. Thouvenin, C. Gaquiere, N. Vellas, and J.-F. Lampin, High performance heterostructure low barrier diodes for sub-THz detection, *IEEE Trans. Terahertz Sci. Technol.* **7**, 780–788 (2017), <https://doi.org/10.1109/TTHZ.2017.2755503>
- [23] M. Lee, L.N. Pfeiffer, and K.W. West, Ballistic cooling in a wideband two-dimensional electron gas bolometric mixer, *Appl. Phys. Lett.* **81**, 1243–1245 (2002), <https://doi.org/10.1063/1.1500429>
- [24] V. Palenskis, L. Minkevičius, J. Matukas, D. Jokubauskis, S. Pralgauskaitė, D. Seliuta, B. Čechavičius, R. Butkutė, and G. Valušis, InGaAs diodes for terahertz sensing—effect of molecular beam epitaxy growth conditions, *Sensors* **18**, 1–15 (2018), <https://doi.org/10.3390/s18113760>
- [25] D. Pashnev, V.V. Korotyeyev, J. Jorudas, A. Urbanowicz, P. Prystawko, V. Janonis, and I. Kasalynas, Investigation of electron effective mass in AlGa_N/Ga_N heterostructures by THz spectroscopy of Drude conductivity, *IEEE Trans. Electron Devices* **69**, 3636–3640 (2022), <https://doi.org/10.1109/TED.2022.3177388>
- [26] J.K. Choi, V. Mitin, R. Ramaswamy, V.A. Pogrebnyak, M.P. Pakmehr, A. Muravjov, M.S. Shur, J. Gill, I. Mehdi, B.S. Karasik, and A.V. Sergeev, THz hot-electron micro-bolometer based on low-mobility 2-DEG in Ga_N heterostructure, *IEEE Sens. J.* **13**, 80–88 (2013), <https://doi.org/10.1109/JSEN.2012.2224334>
- [27] E. Šermukšnis, J. Jorudas, A. Šimukovič, V. Kovalevskij, and I. Kašalynas, Self-heating of annealed Ti/Al/Ni/Au contacts to two-dimensional electron gas in AlGa_N/Ga_N heterostructures, *Appl. Sci.* **12**, 11079 (2022), <https://doi.org/10.3390/app122111079>
- [28] J. Jorudas, J. Malakauskaite, L. Subacius, V. Janonis, V. Jakstas, V. Kovalevskij, and I. Kasalynas, Development of the planar AlGa_N/Ga_N bow-tie diodes for terahertz detection, in: *Proceedings of the 2019 44th International Conference on Infrared, Millimeter, and Terahertz Waves (IEEE, 2019)* pp. 1–2, <https://doi.org/10.1109/IRMMW-THz.2019.8873816>
- [29] J. Jorudas and I. Kasalynas, Terahertz responsivity of AlGa_N/Ga_N bow-tie diode detectors at the temperatures of 295 K and 80 K, in: *Proceedings of the 2022 47th International Conference on Infrared, Millimeter, and Terahertz Waves (IEEE, 2022)* pp. 1–2, <https://doi.org/10.1109/IRMMW-THz50927.2022.9895472>
- [30] S. Pralgauskaitė, J. Matukas, E. Kažukauskas, I. Kašalynas, V. Janonis, and P. Prystawko, Low

frequency noise spectroscopy of GaN bow-tie THz detectors, in: *Proceedings of the 25th International Conference on Noise Fluctuations (ICNF 2019)*, ed. C. Enz (ICLAB, Neuchâtel, Switzerland, 2019), <https://doi.org/10.5075/epfl-ICLAB-ICNF-269187>

[31] M. Bauer, A. Ramer, S.A. Chevtchenko, K.Y. Osipov, D. Cibiraite, S. Pralgauskaitė, K. Ikamas,

A. Lisauskas, W. Heinrich, V. Krozer, and H.G. Roskos, A high-sensitivity AlGaIn/GaN HEMT terahertz detector with integrated broadband bow-tie antenna, *IEEE Trans. Terahertz Sci. Technol.* **9**, 430–444 (2019), <https://doi.org/10.1109/TTHZ.2019.2917782>

ASIMETRIŠKAI SUSIAURINTŲ AlGaIn/GaN HETEROSTRUKTŪRŲ PETELIŠKĖS TIPO DIODAI TERAHERCINIAM DAŽNIŲ RUOŽUI

J. Jorudas^a, D. Seliuta^a, L. Minkevičius^a, V. Janonis^a, L. Subačius^a, D. Pashnev^a, S. Pralgauskaitė^a, J. Matukas^a, K. Ikamas^b, A. Lisauskas^b, E. Šermukšnis^c, A. Šimukovič^c, J. Liberis^c, V. Kovalevskij^d, I. Kašalynas^{a,b}

^a *Fizinių ir technologijos mokslų centro Terahercų fotonikos laboratorija, Vilnius, Lietuva*

^b *Vilniaus universiteto Taikomosios elektrodinamikos ir telekomunikacijų institutas, Vilnius, Lietuva*

^c *Fizinių ir technologijos mokslų centro Fluktuacinių reiškinių laboratorija, Vilnius, Lietuva*

^d *Fizinių ir technologijos mokslų centro Eksperimentinės branduolio fizikos laboratorija, Vilnius, Lietuva*

Santrauka

Asimetriškai susiaurintos AlGaIn/GaN heterostruktūros su laidžiu dvimačių elektronų dujų (2DEG) sluoksniu panaudotos sukurti peteliškės tipo (BT) diodus, tinkančius terahercinio dažnių ruožo (THz) bangoms registruoti kambario temperatūroje. Atsižvelgiant į tai, kad be išorinės postūmio įtampos THz BT diodo veikimas yra labiau tinkamas praktiniams taikymams, ištyrėme diodus su didele srovės ir įtampos (IV) charakteristikų asimetrija, kuri buvo tuo ryškesnė, kuo mažesnis kakliuko plotis, parodant didelį diodų jautrumą THz bangoms. Krūvininkų kaitinimas metalizuotame diodo lapelyje buvo išskirtas kaip pagrindinis mechanizmas, lemiantis THz bangų lyginimą BT diode. Jautris ir triukšmo ekvivalentinė galia (NEP) ties pagrindiniu antenos dažniu 150 GHz siekė iki 4 V/W ir atitinka-

mai 2 nW/ $\sqrt{\text{Hz}}$. Toks didelis BT diodų jautrumas leido mums pirmą kartą išmatuoti asimetrinės BT antenos dažninę charakteristiką, stebint pagrindinį ir aukštesnės eilės antenos rezonansus, parodant gerą sutapimą su baigtinių skirtumų laiko skalėje atliktais modeliavimo rezultatais plačiame dažnių ruože. Išsamus AlGaIn/GaN BT diodų žemo ir aukšto dažnio triukšmo charakteristikų tyrimas atskleidė, kad nenaudojant įtampos postūmio reikia atsižvelgti tik į šiluminį triukšmą, kurio vertė buvo santykinai maža dėl didelio 2DEG tankio, lemiančio nedidelę diodo varžą. Taip pat nustatėme, kad BT diodo jautrumas netiesiniu dėsniu priklauso nuo jo varžos, dėl to diodo kakliuko siaurinimas žemiau kelių mikronų vertės gali būti mažai veiksmingas, kai tikimasi mažų NEP verčių.